Journal Name

From instantaneous normal modes to parameter-free predictions of the viscoelastic response of glassy polymers

Vladimir V. Palyulin[a], Christopher Ness[a], Rico Milkus[a], Robert M. Elder[bc], Timothy W. Sirk[b†], Alessio Zaccone[a*]

We study the viscoelastic response of amorphous polymers using theory and simulations. By accounting for internal stresses and considering instantaneous normal modes (INMs) within athermal non-affine theory, we make parameter-free predictions of the dynamic viscoelastic moduli obtained in coarse-grained simulations of polymer glasses at non-zero temperatures. The theoretical results show excellent correspondence with simulation data over the entire domain of frequency of externally applied shear, with only minor instabilities that accumulate in the low-frequency part on approach to the glass transition. These results provide evidence that the mechanical glass transition itself is continuous and thus represents a crossover rather than a true phase transition. The relatively sharp drop of the low-frequency storage modulus across the glass transition temperature can be explained mechanistically within the proposed theory: the proliferation of low-eigenfrequency vibrational excitations (boson peak and nearly-zero energy excitations) is directly responsible for the rapid increase (in absolute value) of the negative non-affine contribution to the storage modulus.

Introduction

A predictive framework for the viscoelastic properties of amorphous polymers has remained out of reach to date. We show that an athermal atomistic deformation theory suitably modified to account for instantaneous normal modes is able to make parameter-free predictions of the viscoelastic moduli over the whole range of shear oscillation frequencies and across a broad temperature range even above the glass transition. Our approach also provides a new insight into the microscopic changes that occur at the onset of the mechanical glass transition. The theoretical predictions are intensively and successfully tested against the dynamic mechanical response results obtained by molecular dynamics simulations for coarse-grained polymers.

In idealised crystals at low temperature the lattice inversion symmetry ensures that atoms are displaced homogeneously under applied deformation, i.e. all displacements are *affine*. The sum of forces on each atom in the deformed configuration is thus zero thanks to centrosymmetry, leading to straightforward determination of the elastic properties[1]. Amorphous solids, in contrast, lack such symmetry, and rather exhibit a static snapshot configuration closer to that of liquids. As a consequence, net remnant forces under shear displace the atoms from their affine positions, causing the so-called *non-affine* deformation (Fig.). Except at infinite frequency of applied shear, where this non-affine relaxation is inhibited, classical affine microscopic theory fails to predict the mechanical deformation behaviour of amorphous solids[2].

Recent works address this shortcoming using theoretical models based principally on solutions of the equation of motion for the non-affine displacement of a tagged atom[2–5]. A correction to the stress response can be obtained[2] by enforcing mechanical equilibrium on every atom at all steps in the deformation: the forces arising when nearest-neighbour atoms try to find their affine position are relaxed at all steps, and the displacement field which satisfies the mechanical equilibrium contains additional *non-affine* displacements on top of the affine ones. This non-affine deformation framework is crucially dependent on the vibrational density of states (VDOS), since one needs to evaluate this force-relaxation over the whole space of degrees of freedom, and on

[a] Department of Chemical Engineering and Biotechnology, University of Cambridge, Cambridge, CB3 0AS, United Kingdom

[b] Polymers Branch, U.S. Army Research Laboratory, Aberdeen Proving Ground, Maryland 21005, USA.

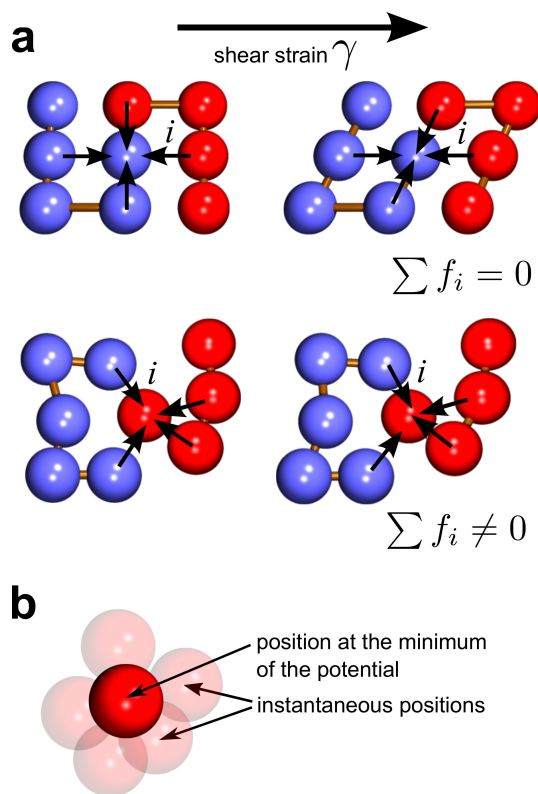[c] Bennett Aerospace, Inc., Cary, North Carolina 27511, USA

† E-mail: timothy.w.sirk.civ@mail.mil

* E-mail: az302@cam.ac.uk

a quantity which describes how the force field due to affine displacements depends on eigenfrequency[2,6]. Both the VDOS and the eigenmode-correlator of the affine force-field are found by diagonalization of the Hessian matrix of the system. Importantly, the low-frequency part of the VDOS makes the most substantial contribution to the viscoelastic moduli, which is consistent with the observation of anomalous soft modes in glasses[7–9]. These modes arise from the lowest energy barriers for rearrangements of atoms[10–12].

The non-affine deformation framework as described above assumes that the system is athermal. Practically, this means that the system resides at, or very close to, a local minimum of the potential energy, fluctuations are negligible, and features of the behaviour are described by standard normal mode analysis. In reality, however, the system spends most of its time off the energy minimum even at low non-zero temperatures. One approach to the computation of the VDOS in this case is based on instantaneous normal modes (INM)[13,14]. Instead of using the energy of the system at the potential minimum as in conventional normal mode analysis, single snapshots of the system are considered and averaging is performed over the snapshots. This method was earlier applied to liquids[15] as well as glassy systems such as LJ glass[16], silica[17] and proteins[18]. The instantaneous normal modes of liquids have predictive power only at high frequencies[19–21]. For amorphous solids these modes can be defined at much slower timescales, i.e. some properties of solids as well as the glass transition can be associated with INMs[22].

In this work we show that a combination of the non-affine theory and the INM approach produces quantitative parameter-free predictions for viscoelastic behavior of amorphous solids. We compute the VDOS and correlators of affine forces from averages over snapshots of the system rather than from a long-time average, which is necessary for taking the temperature-dependent unstable modes into account[14]. As a model system we use polymer glasses. However, the method and the results are relevant far beyond this particular system. Our choice is based on high practical relevance of polymer materials and the fact that their complexity better highlights the usefulness of the theory. Remarkably, viscoelastic moduli G' and G'' computed within our framework match results from numerical simulations not just for the athermal (very low temperature) case, but across a wide range of temperatures extending even above the glass transition temperature into the liquid state.

$$\sum f_i = 0$$

$$\sum f_i \neq 0$$

position at the minimum of the potential

instantaneous positions

As temperature is increased, the system spends more time further away from local potential energy minima[23], leading to increased importance of INMs as well as local internal stresses (because away from the minimum the first derivative of intermolecular interaction is non-zero). Once the internal stresses are included, the analysis produces some negative eigenvalues, which correspond to imaginary frequencies in the VDOS and therefore to non-propagating relaxation modes down from saddles (these modes are localilzed). The number and the density of these relaxation modes grow with temperature, reflecting an increasing instability of the system. Importantly, this growth is continuous across the glass transition, providing evidence that the glass transition, at least in its mechanical manifestations, has hallmarks of a crossover rather than a true phase transition. As such, our approach offers fundamental insights into the mechanics of amorphous materials across the glass transition, as well as a robust prediction of the viscoelastic properties of real amorphous materials across both solid and liquid states.

0ptTheory and Simulations

We focus on the case of small deformations, within the regime of linear viscoelasticity and avoiding complications such as shear banding[24], local anharmonicity and nonlinear plastic modes[25,26], all of which lie out of the scope of our approach. Our formalism below is written accordingly. The non-affine theory[2–4] computes corrections to the elastic moduli due to additional displacements caused by an extra net force from neighbors in the case of non-centrosymmetric materials (Fig.). The non-affine displacements cause softening of the material. The corresponding correction to the elastic free energy is negative and for shear deformation it
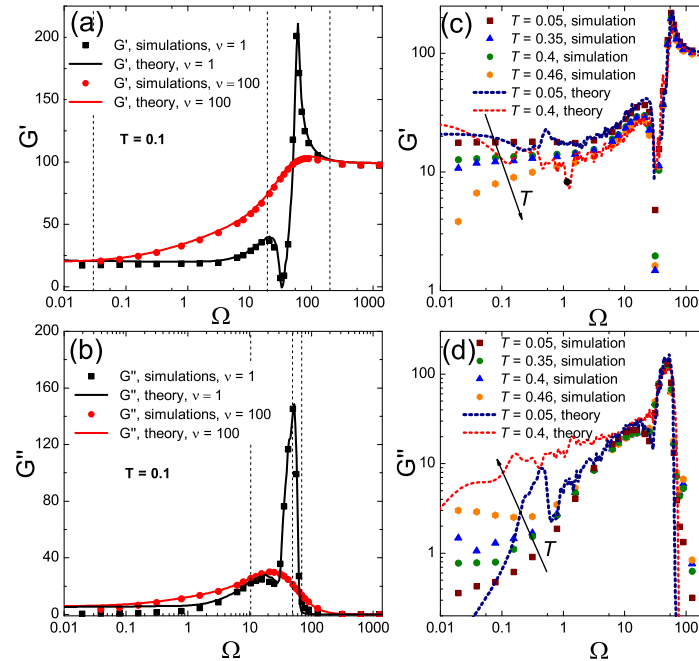
can be expressed as

$$F = F_A - F_{NA} = F_A - \frac{1}{2}\sum_i \frac{\partial \mathbf{f}_i}{\partial \gamma}\frac{\partial \mathbf{r}_i}{\partial \gamma}\gamma^2, \qquad (1)$$

where the affine part F_A was given already by Born and Huang[1], γ is a shear angle (shear strain amplitude), $\mathbf{f}_i$ is the net force which acts on the atom i in its affine position (see Fig. 1), $\mathbf{r}_i$ is radius-vector to i-th atom, F_{NA} is the non-affine contribution to free energy. If the interactions between the atoms are described by harmonic central forces then Eq. 1 can be written as[27]

$$F = F_A - \frac{1}{2}\mathbf{\Xi}_i H_{ij}^{-1}\mathbf{\Xi}_j\gamma^2, \qquad (2)$$

where an affine force field $\mathbf{\Xi}_i$ is responsible for a force $\mathbf{f}_i = \mathbf{\Xi}_i\gamma$ acting on atom i, and H_{ij} is the Hessian (which for a system of N particles has size $3N \times 3N$), which includes the internal stresses induced by thermal fluctuations via the INMs (for details see SI). Summation over repeated indices is implied. Assuming the system dwells in the vicinity of a local energy minimum, the microscopic equation of motion for a particle of mass m can be written as that of a damped harmonic oscillator

$$m\ddot{\mathbf{r}}_i + \nu\dot{\mathbf{r}}_i + H_{ij}\mathbf{r}_j = \mathbf{\Xi}_i\gamma, \qquad (3)$$

where the second term characterises energy dissipation due to viscous damping (with friction coefficient ν), the third term is the harmonic force pulling the particle back into the minimum and the right hand side is the non-affine force, which depends on the shear amplitude γ.

Transformation of Eq. (3) into Fourier space allows us to obtain an expression for the complex viscoelastic modulus, which in the continuous limit reads (see SI for more details)

$$G^*(\Omega) = G' + iG'' = G_A - \frac{1}{V}\int_0^{\omega_D} D(\omega)\frac{\Gamma(\omega)}{m\omega^2 - m\Omega^2 + i\Omega\nu}, \qquad (4)$$

where Ω is the applied strain frequency, $\Gamma(\omega) = \langle\mathbf{\Xi}^2\rangle_{\omega\in[\omega,\omega+d\omega]}$ is the affine force field correlator in terms of normal-mode decomposed vector $\mathbf{\Xi}$, defined as in[2], which tells the degree of correlation of affine forces in the eigenfrequency shell, and G_A is the affine contribution[1]. The important quantity, which implicitly enters the expression, is the vibrational density of states $D(\omega)$. The inputs to the expression for $G^*(\Omega)$ are the eigenvalues (through ω) and eigenvectors (through $\Gamma(\omega)$) of the Hessian matrix H_{ij}, which we obtain from molecular simulations of glassy polymer configurations as described in the following.

Amorphous polymeric systems of $N = 50$ and 100 linear homopolymer chains with polymerisation degree 100 were modelled in a periodic domain using LAMMPS[28]. We adopt the conventional Kremer-Grest bead-spring model[29], i.e. polymer backbone covalent bonds were simulated using a finitely-extensible nonlinear elastic (FENE) potential, while non-bonding interactions were represented by a shifted Lennard-Jones (LJ) pair potential. For the FENE potential $U_{FENE} = -0.5KR_0^2\ln\left[1 - \left(\frac{r}{R_0}\right)^2\right]$ the parameters were set as $K = 30, R_0 = 1.5$. For LJ potential $U_{LJ} = 4\varepsilon\left[\left(\frac{\sigma}{r_c}\right)^{12} - \left(\frac{\sigma}{r_c}\right)^6\right]$ the constants were chosen to be $\varepsilon = 1$ and the cutoff radius $r_c = 2.5$ (which matches that used in the computation of H_{ij}). Bead trajectories are updated according to Langevin dynamics, with a damping constant ξ (which is related to the theoretical damping term by $\xi = m/\nu$). ε sets the LJ energy scale, and K is the bond energy scale, where $K/\varepsilon = 30$. With reference to fundamental units of mass M, length d and energy ε we set $\sigma = 1$ and $m = 1$, giving a time unit of $\tau = \sqrt{m\sigma^2/\varepsilon}$. We equilibrate the system in a melted state at $T^* = 1.0$, maintaining zero external pressure using a Nose-Hoover barostat. We then cool the system by decreasing T^* with a characteristic timescale $\tau_c = 10^5\tau$.

We then obtain the viscoelastic moduli by mechanical spectroscopy, applying a small amplitude oscillatory simple shear strain to the sample as in Refs. [5,30]. From the stress-strain curves we compute the storage G' and loss G'' moduli

$$G' = \frac{\sigma_0}{\varepsilon_0}\cos\delta, G'' = \frac{\sigma_0}{\varepsilon_0}\sin\delta, \qquad (5)$$

where σ_0 is the average amplitude of stress, ε_0 is the amplitude of strain (fixed at 2%) and δ is a phase shift between the two.
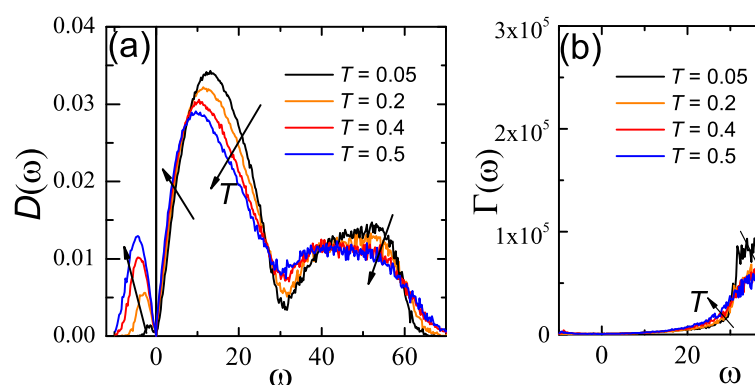
Viscoelastic moduli

Using the methods described in the previous section we first compare theoretical predictions of G' and G'' (obtained using instantaneous static simulation snapshots to form the VDOS with INM) against simulation results obtained by mechanical spectroscopy for low temperature, $T = 0.1$. Fig. 2(a,b) shows the storage (A) and loss (B) moduli for low and high internal friction ν (cf Eq. 4 and ξ in simulation description), respectively. For the correspond-

ing friction coefficients, the theory provides a good quantitative prediction of the mechanical spectroscopy data (continuous lines and symbols, respectively, in Fig. 2(a,b)) without any fitting or adjustable parameter.

The peaks in $G'(\Omega)$ (Fig. 2(a)) correspond to the strongest resonances in the system. The highest peak is located close to the resonance frequency of FENE bonds $\omega_{\text{FENE}} \approx 31.3$, while the peak at lower frequencies is located between the FENE bond peak and the LJ resonance frequency ($\omega_{\text{LJ}} \approx 7.56$). Between the peaks G' falls to very small values. With an increase of the friction, the transition from the high frequency regime to low frequency regime is smoother, with resonances being smeared off. At very low frictions (not shown) the theoretical curves show a number of small single frequency resonances, consistent with low temperature results produced by non-affine theory without INMs for amorphous silica glasses[5]. In our case the friction is constant (Markovian) by construction of the molecular simulations with Langevin thermostat, and not a function of Ω. In some real materials such as metallic glass this may not be the case, and an extension that includes memory-function for the friction has been reported recently[31].

Increasing T mostly affects the values of the moduli at low frequency, shown in Fig. 2 (c,d). The storage modulus drops substantially after the temperature exceeds the glass transition temperature $T_g = 0.4$, i.e. upon "disorder-assisted" melting[4]. On the contrary, the loss modulus grows with temperature, which also reflects a growth in dissipation defined usually as G''/G'. The glass transition temperature T_g of our system, which we determined earlier from the change of thermal expansion coefficient for this system[32], is consistent with the behaviour of the moduli at low frequencies. The data from simulations for low frequency $\Omega = 0.03$ (Fig. 2(e)) show that G' drops significantly at $T \approx 0.4$ and thereafter smoothly tends to zero, which is consistent with recent results[33,34] obtained from the stress-fluctuation formalism[35]. In order to compare the theory with simulation data at different temperatures we have plotted values of the storage modulus for high frequencies and intermediate frequencies in Fig. 2(e). We see that the theory is able to predict the storage modulus even in the liquid phase for moderate to high oscillation frequencies Ω. Fig. 2(f) shows the comparison of theoretical and simulation data for the loss modulus. Since at very low and very high frequencies the values of G'' become very small and rather noisy, we have chosen a set of frequencies different from that used for the plot of the storage modulus (Fig. 2(e)). We observe that the match between the theoretical predictions and the simulation data is less quantitatively accurate, but is qualitatively good at intermediate and high frequencies.

Although the non-affine approach was developed originally for the athermal case[2,27], the success of its predictions shown in Figs 2(a,b,e,f) suggests that our inclusion of INMs and internal stresses makes it applicable over a very broad range of temperature, even above T_g. We have checked that, upon computing the VDOS in the standard way, i.e. by taking configurations from long time energy-minimised simulations (which washes out the relaxation modes and the internal stresses), the comparison with simulation data is much worse.

With an increase of T to a value close or above T_g, the predictions of INM non-affine theory get less quantitatively accurate at low frequency (see Fig 2(e)). We believe that a growing mismatch with mechanical spectroscopy data is caused by the increased anharmonicity and by swaps of nearest-neighbours. Even at non-zero temperatures for moderate and high frequencies of shearing, the atoms mostly dwell around their local minima, hence the harmonic approximation holds, although internal stresses resulting from displacements off the minima are important and are taken into account via the INM in our theory. Increase of the external force period (for $\Omega \ll 1$) leads to the increase of atom mobility, because the atoms have more time to relax their positions with respect to their neighbors. Indeed, in the SI we show results illustrating that the number of nearest neighbor changes increases with period and temperature. Moreover, we observe a crossover to a more active increase in number of swaps of nearest neighbors once the temperature exceeds T_g. Since these swaps are not taken into account in Eq. (3), some mismatch arises at the very lowest frequencies once $T > T_g$.

Analysis of vibrational excitations

If the Hessian matrix is computed for instantaneous atom positions instead of positions taken from a minimised energy state of the system, then the diagonalization of **H** produces negative eigenvalues[13,14,37]. Their presence indicates that the local slope and curvature of the energy hypersurface has nonconvex components, so the density of these modes is linked to non-propagating relaxation from local saddles (produced by thermal excitation) in the energy landscape[13]. Since the instantaneous positions deviate more from their rest positions as the temperature is increased, the behaviour of the negative eigenvalues, which correspond to

imaginary frequencies, correlates with softening of the material and the transition from solid-like to liquid-like properties.

In Fig. 3(a) we plot the overall fraction of vibrational modes that are negative as function of temperature. The behavior of unstable modes is rather similar to silica glasses from Ref. [17] and the small protein system from Ref. [18]: they appear once the temperature gets above zero. This fraction could also be obtained by the ratio of the areas of imaginary part of VDOS to the real one (see Fig. 3(b)). To understand the nature of these negative modes, we compute a standard measure of localization, the participation ratio $p(\omega_j)$. For an eigenmode with the eigenfrequency ω_j, it is defined as:
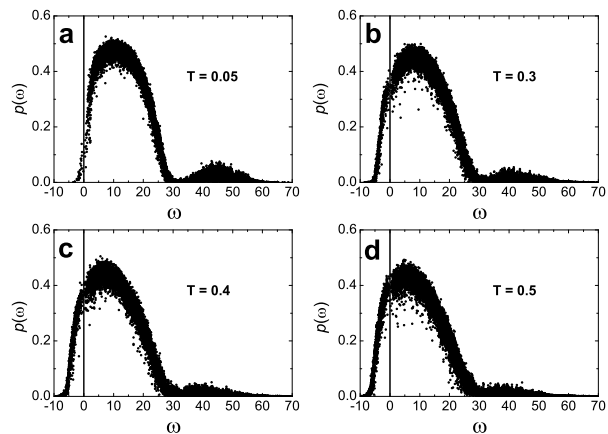
$$p(\omega_j) = \frac{\left(\sum_{i=1}^{N} u_i^2(\omega_j)\right)^2}{N \sum_{i=1}^{N} u_i^4(\omega_j)}, \qquad (6)$$

where $u_i(\omega_j)$ is the total amplitude of the i-th atom's eigenvector. $p(\omega_j)$ quantifies the number of particles participating in a single mode. For instance, for an isolated particle one has $p = 1/N$, while if all particles are involved in a single mode $p = 1$. For an amorphous polymer solid, which we consider here, the participation ratio shows substantial change with an increase in temperature (Fig. 4).

As is customary [13], we show imaginary frequencies as negative ones. For low temperature ($T = 0.05$) almost all frequencies are real. As the temperature approaches and crosses T_g, more modes become unstable. At around T_g the shoulder of the first band of participation ratio (with values 0.4-0.5) is crossing into the unstable domain, but there is no special feature visible at $T_g = 0.4$ and the process appears smooth across the glass transition. This calculation also shows that the unstable relaxation modes are localized, with low values of participation ratio of imaginary-frequency modes.

One can notice that even for the data at the lowest temperature $T = 0.05$ the participation ratio at low (real) frequencies has values around 0.2-0.4, i.e. the long-wavelength phonons, which are supposed to have $p \approx 0.6$, are not apparent. This does not mean, however, that the phonons are not present. The necessary truncation of the system size in simulations often leads to small values of $p(\omega)$ at the phonon frequencies, which is not unusual for delocalized modes [38]. Interestingly, just like in the case of dependence of viscoelastic moduli on the temperature, there are no obvious signatures of a transition in $p(\omega)$ at or near T_g.

This corroborates the seminal idea of Y. Frenkel [36], that, in the case of amorphous solids, there is a continuity between the liquid and solid states at least for the mechanical properties, and that, indeed, liquids behave like solid glasses at sufficiently high frequency of deformation.

On the microscopic scale, the viscoelastic properties are controlled by the vibrational density of states $D(\omega)$ and affine force field $\Gamma(\omega)$ (see Eq. 4), both of which contribute to non-affine softening. The density of vibrational states for a polymer amorphous solid at low temperatures consists of two prominent features (Fig. 3(b)): a large peak upon normalizing by Debye's $\sim \omega^2$ law, the so-called 'boson peak', which is associated with LJ interactions between beads; and a plateau at higher frequencies corresponding to FENE bond and collective bond-LJ vibrations [39,40]. The boson peak can be measured by neutron inelastic scattering experiments for instance for polyethylene [41] or PDMS [42].

An increase of temperature leads to the shift of boson peak and the FENE-bond plateau to lower frequencies (Fig. 3(b)), which increases the non-affine contribution (see Eq. 4) and, thus, makes the material softer. The increase of the boson peak and its shift to lower frequencies clearly gives rise to an increase (in absolute value) of the non-affine integral due to the weight in the denominator which gives high weight to the low-ω part of the VDOS.

$\Gamma(\omega)$ also increases strongly in the range of $20 \leq \omega \leq 30$ (Fig. 3(c)). The large amplitude and fluctuations of $\Gamma(\omega)$ in the high frequency part does not play a significant role for non-affine contributions due to the fast growth of $1/\omega^2$ part in the integrand in Eq. 4. Thus, both the density of INMs and the correlator of affine force field show features leading to the softening of the material with increasing T. It is clear that in our case the crossover from solid to liquid state above $T_g = 0.4$ does not bring any new microscopic signatures of a transition, i.e. the microscopic INM-based non-affine approach, here quantitatively validated against simulations, corroborates the idea of gradual and continuous amorphous solid-liquid crossover.

0ptConclusions

Prediction of the dynamic mechanical properties of amorphous solids and liquids proves to be perhaps the most elusive problem in condensed matter and materials physics. Although the experimentally observed properties of solids and liquids are clearly very different, the static snapshot of atomic positions looks the same. We have combined microscopic dynamical information about internal stresses in the form of INMs with the athermal non-affine

deformation theory. The combined approach is capable of describing the viscoelastic properties of polymer glasses at non-zero temperatures up to and beyond the glass transition, across all frequencies. The drop of the low-frequency storage modulus at T_g is *quantitatively* linked with an important growth of the so-called boson peak (proliferation of soft modes above the Debye ω^2 level) in the VDOS and its shift towards zero frequency/energy, and with the gradual appearance of non-propagating, unstable relaxation modes (imaginary eigenfrequencies) already below T_g. All other microscopic features of the vibrational excitations and microscopic dynamics change continuously and gradually across T_g, with no kinks or sharp features. These results strongly support the view of the glass transition as a fundamental continuity between the liquid and the amorphous solid state [43,44], at least for its mechanical manifestations. The predictive framework presented here opens up the way to the chemical-design in silico of new amorphous functional materials with high-performance mechanical properties.

0ptReferences

1 Born M and Huang H (1954) *Dynamical Theory of Crystal Lattices* (Oxford: Oxford University Press).

2 Lemaître, A. & Maloney, C. Sum Rules for the Quasi-Static and Visco-Elastic Response of Disordered Solids at Zero Temperature. *J. Stat. Phys.* **123**, 415-453 (2006).

3 Zaccone, A. & Scossa-Romano, E. Approximate analytical description of the non-affine response of amorphous solids. *Phys. Rev. B* **83**, 184205 (2011). .

4 Zaccone, A. & Terentjev, E. M. Disorder-Assisted Melting and the Glass Transition in Amorphous Solids. *Phys. Rev. Lett.* **110**, 178002 (2013).

5 Damart, T., Tanguy, A., & Rodney, D. Theory of harmonic dissipation in disordered solids. *Phys. Rev. B* **95**, 054203 (2017).

6 Milkus, R. & Zaccone, A. Atomic-scale origin of dynamic viscoelastic response and creep in disordered solids. *Phys. Rev. E* **95**, 023001 (2017).

7 Franz, S., Parisi, G., Urbani, P., & Zamponi, F., Universal spectrum of normal modes in low-temperature glasses. *Proc. Natl. Acad. Sci. USA* **112**, 14539-14544 (2015).

8 Xu, N., Vitelli, V., Liu, A. J. & Nagel, S. R. Anharmonic and quasi-localized vibrations in jammed solids modes for mechanical failure. *Europhys. Lett.* **90**, 56001 (2010).

9 DeGiuli, E., Laversanne-Finot, A., Düring, G., Lerner, E. & Wyart, M. Effects of coordination and pressure on sound attenuation, boson peak and elasticity in amorphous solids. *Soft Matter* **10**, 5628-5644 (2014).

10 Brito, C. & Wyart, M. Geometric interpretation of previtrification in hard sphere liquids. *J. Chem. Phys.* **131**, 024504 (2009).

11 Manning, M.L. & Liu, A.J. Vibrational modes identify soft spots in a sheared disordered packing. *Phys. Rev. Lett.* **107**, 108302 (2011).

12 Dasgupta, R., Karmakar, S. & Procaccia, I. Universality of the plastic instability in strained amorphous solids. *Phys. Rev. Lett.* **108**, 075701 (2012).

13 Stratt, N.M. The Instantaneous Normal Modes of Liquids. *Acc. Chem. Res.* **28**, 201-207 (1995).

14 *Normal Mode Analysis. Theory and applications to biological and chemical systems* (2006) (Eds. Cui Q and Bahar I, Chapman & Hall/CRC Mathematical and Computational Biology)

15 Keyes, T. Instantaneous Normal Mode Approach to Liquid State Dynamics. *J. Phys. Chem. A* **101**, 2921-2930 (1997).

16 Bembenek, S. D. & Laird, B. B. The role of localization in glasses and supercooled liquids. *J. Chem. Phys.* **104**, 5199-5208 (1996).

17 Bembenek, S. D. & Laird, B. B. Instantaneous normal modes analysis of amorphous and supercooled silica. *J. Chem. Phys.* **114**, 2340-2344 (2001).

18 Schulz, R., Krishnan, M., Daidone, I. & Smith, J.C. Instantaneous Normal Modes and the Protein Glass Transition. *Biophys. J.* **96**, 476-484 (2009).

19 Gezelter, J.D., Rabani, E., & Berne, B.J. Can imaginary instanteneous normal mode frequencies predict barriers to self-diffusion? *J. Chem. Phys.* **107**, 4618-4627 (1997).

20 Stratt, R.M., The relationship between the elastic constants and the instantaneous normal modes of liquids. *International Journal of Thermophysics* **18**, 899-907 (1997).

21 David, E.F. & Stratt R.M., The anharmonic features of the short-time dynamics of fluids: The time evolution and mixing of instantaneous normal modes. *J. Chem. Phys.* **109**, 1375-1388 (1998).

22 Bembenek, S. D. & Laird, B. B. Instanteneous normal modes and the glass transition. *Phys. Rev. Lett.*, **74**, 936-939 (1995).

23 Goldstein, M. Viscous Liquids and the Glass Transition: A Potential Energy Barrier Picture. *J. Chem. Phys.* **51**, 3728-3739 (1969).

24 Parisi, G., Procaccia, I., Rainone. C. & Singh, M. Shear bands as manifestation of a criticality in yielding amorphous solids. *Proc. Natl. Acad. Sci. USA 114*, 5577-5582 (2017).

25 Lerner, E. The micromechanics of nonlinear plastic modes. *Phys. Rev. E* **93**, 053004 (2016).

26 Zylberg, J., Lerner, E., Bar-Sinai, Y. & Bouchbinder, E. *Proc. Natl. Acad. Sci. USA 114*, 7289-7294 (2017).

27 Lutsko, J. F. Generalized expressions for the calculation of elastic constants by computer simulation. *Journal of Applied Physics* **65**, 2991-2997 (1989).

28 Plimpton, S. Fast Parallel Algorithms for Short-Range Molecular Dynamics. *J. Comp. Phys.* **117**, 1-19 (1995). See also: http://lammps.sandia.gov

29 Grest, G. S. & Kremer, K. Molecular dynamics simulation for

polymers in the presence of a heat bath. *Phys. Rev. A* **33**, 3628-3631 (1986).

30 Ranganathan, R., Shi, Y. & Keblinski, P. Frequency-dependent mechanical damping in alloys. *Phys. Rev. B* **95**, 214112 (2017).

31 Cui, B., Yang, J., Qiao, J., Jiang, M., Dai, L., Wang, Y. J. & Zaccone, A. Atomic theory of viscoelastic response and memory effects in metallic glasses. *Phys. Rev. B* **96**, 094203 (2017).

32 Ness, C., Palyulin, V. V., Milkus, R., Elder, R., Sirk, T. & Zaccone, A. Nonmonotonic dependence of polymer-glass mechanical response on chain bending stiffness. *Phys. Rev. E* **96**, 030501(R) (2017).

33 Kriuchevskyi, I., Wittmer, J. P., Meyer, H. & Baschnagel, J. Shear modulus and shear-stress fluctuations in polymer glasses. *Phys. Rev. Lett.* **119**, 147802 (2017).

34 Kriuchevskyi, I., Wittmer, J. P., Meyer, H., Benzerara, O. & Baschnagel, J. Shear-stress fluctuations and relaxation in polymer glasses. *Phys. Rev. E* **97**, 012502 (2018).

35 Wittmer, J. P., Xu, H. & Baschnagel, J. Shear-stress relaxation and ensemble transformation of shear-stress autocorrelation functions. *Phys. Rev. E* **91**, 022107 (2015).

36 Frenkel, J. *Kinetic Theory of Liquids* (Oxford University Press, 1947).

37 Keyes, T. Unstable modes in supercooled and normal liquids: Density of states, energy barriers, and self-diffusion. *J. Chem. Phys.* **101**, 5081-5092 (1994).

38 Mazzacurati, V., Ruocco, G. & Sampoli, M. Low-frequency atomic motion in a model glass. *Europhys. Lett.* **34**, 681-686 (1996).

39 Jain, T. S. & de Pablo, J. J. Influence of confinement on the vibrational density of states and the Boson peak in a polymer glass. *J. Chem. Phys.* **120**, 9371-9375 (2004).

40 Milkus, R., Ness, C., Palyulin, V.V., Weber, J., Lapkin, A., & Zaccone A. Interpretation of the Vibrational Spectra of Glassy Polymers Using Coarse-Grained Simulations. *Macromolecules*, 10.1021/acs.macromol.7b02352

41 Kanaya, T., Kaji, T., Ikeda, S., Inoue, K. Low-energy excitations in polyethylene: Comparison between amorphous and crystalline phases. *Chem. Phys. Lett.* **150**, 334-338 (1998).

42 Schönhals, A., Zorn, R., Frick, B. Inelastic neutron spectroscopy as a tool to investigate nanoconfined polymer systems. *Polymer* **105**, 393-406 (2016).

43 Trachenko, K., Brazhkin, V. V. Collective modes and thermodynamics of the liquid state. *Rep. Prog. Phys.* **79**, 016502 (2016).

44 Yang, C., Dove, M. T., Brazhkin, V. V., Trachenko, K. Emergence and Evolution of the k Gap in Spectra of Liquid and Supercritical States. *Phys. Rev. Lett.* **118**, 215502 (2017).